Theor Chem Acc (2002) 108:232–239
DOI 10.1007/s00214-002-0381-7

Theoretical
Chemistry Accounts

*Regular article*

# Density functional theory study of the mechanism of the proline-catalyzed intermolecular aldol reaction

**Manuel Arnó, Luis R. Domingo**

Instituto de Ciencia Molecular, Departamento de Química Orgánica, Universidad de Valencia, Dr. Moliner 50, 46100 Burjassot, Valencia, Spain

Received: 2 April 2002 / Accepted: 18 July 2002 / Published online: 11 October 2002


**Abstract.** Transition structures associated with the C—C bond-formation step of the proline-catalyzed intermolecular aldol reaction between acetone and isobutyraldehyde have been studies using density functional theory methods at the B3LYP/6-31G** computational level. A continuum model has been selected to represent solvent effects. For this step, which is the stereocontrolling and rate-determining step, four reactive channels corresponding to the syn and anti arrangement of the active methylene of the enamine relative to the carboxylic acid group of L-proline and the re and si attack modes to both faces of the aldehyde carbonyl group have been analyzed. The B3LYP/6-31G** energies are in good agreement with experiment, allowing us to explain the origin of the catalysis and stereoselectivity for these proline-catalyzed aldol reactions.

**Key words:** Proline catalyst – Aldol reaction – Mechanisms – Transition structures

## 1 Introduction

The aldol reaction is widely regarded to be one of the most important C—C bond-formation reactions utilized in organic chemistry [1, 2, 3, 4, 5]. As a result of its utility, extensive efforts have been applied to the development of catalytic enatioselective variants of this reaction. Catalytic asymmetric aldol reactions are typically accomplished with enolates and chiral transition-metal catalysts [6, 7, 8, 9, 10] or with natural aldolase enzymes [11, 12, 13]. Catalytic antibodies that employ enamine intermediates for aldol reactions have recently been discovered [14, 15, 16, 17, 18, 19].

The capability of a simple organic molecule from the "chiral pool" to act like an enzyme has been shown recently by List et al. [20]. They found that L-proline (**3**) can act as a catalyst for the asymmetric aldol reaction between acetone (**1**) and a wide variety of aldehydes. Yields and enantioselectivities are found to be moderate to good (Scheme 1). This amine-catalyzed asymmetric reaction is conceptually novel and may ultimately lead to new catalysts with higher enantioselectivities [21, 22]. Consequently, the knowledge of the molecular mechanism of these proline-catalyzed aldol reactions is fundamental to understanding the origin of the large catalytic effect and the enantioselectivity in order to select appropriates "micro-aldolases".

The rate-determining step for the antibody aldolases has recently been studied by us in order to characterize the transition-state (TS) analogue for the antibody aldolases. For this step, two channels corresponding to the syn and anti arrangement of the amine hydrogen atom relative to the active methylene group of the enamine have been characterized (Scheme 2). The barrier for the more favorable syn reactive channel via **TS-syn** is 14.8 kcal/mol (MP2/6-31G** calculations). In addition, the syn arrangement is preferred over the anti one, **TS-anti**, by 18.6 kcal/mol, because of the hydrogen-bond formation between the amine hydrogen and the carbonyl oxygen atoms (Scheme 2). This hydrogen-bond increases the electrophilicity of the carbonyl group through a stabilization of the negative charge that is developing at the carbonyl oxygen atom, and favors the formation of the neutral aldol product in one concerted process. Similar

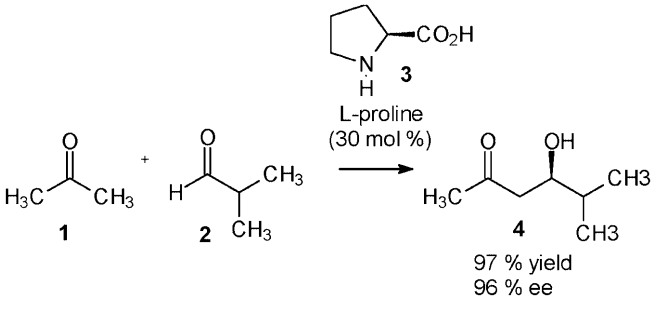


Scheme 1

*Correspondence to*: L. R. Domingo
e-mail: domingo@utopia.uv.es

results have been reported recently by Bahmanyar and Houk [23] for the amine-catalyzed aldol reaction involving enamine intermediates. The activation barrier found for the catalyzed process at the B3LYP/6-31G* level, 14 kcal/mol, is similar to that found by us at the MP2/6-31G** level. While primary enamines give directly the aldol adduct in a concerted fashion, secondary enamine-mediated aldol reactions give zwitterionic intermediates, since there is not a NH group or other proton source to transfer to the developing alkoxide. In consequence, the barrier rises to 33.5 kcal/mol [23].

These studies denote that the hydrogen-bond plays a significant role in stabilizing the developing charges in the TS corresponding with the C—C bond-formation step, decreasing the activation energy of the primary enamine-catalyzed aldol reactions. These results are in agreement with the experimental observation made by Reymond and Chen [24, 25] that primary amines react faster than secondary ones.

For the proline-catalyzed aldol reaction [20] a mechanism closer to that for class I aldolases [14] has been proposed (Scheme 3) [26]. In both cases the formation of enamines **Ia** and **Ib**, respectively, represents the initial step. The addition of these enamine intermediates to an aldehyde and the subsequent release of the catalyst furnishes the aldol product. However, a difference between both catalytic cycles can be seen in the reaction sequence for the formation of the enamines, which are key intermediates of these aldol reactions. In the case of the class I aldolases, a primary amino function of the enzyme is used for the formation of a neutral imine (**IIa**), while the enamine synthesis proceeds through a positive iminium system (**IIb**) when starting from L-proline (Scheme 3). In addition, while the enamine NH hydrogen atom favors the aldol addition in class I aldolases, List et al. [20] have shown that for the catalytic activity of L-proline the carboxylic acid group is required.

In the course of preparing the present manuscript, Bahmanyar and Houk [27] have reported a density functional theory (DFT) study for the origin of the stereoselectivity in the proline-catalyzed intramolecular

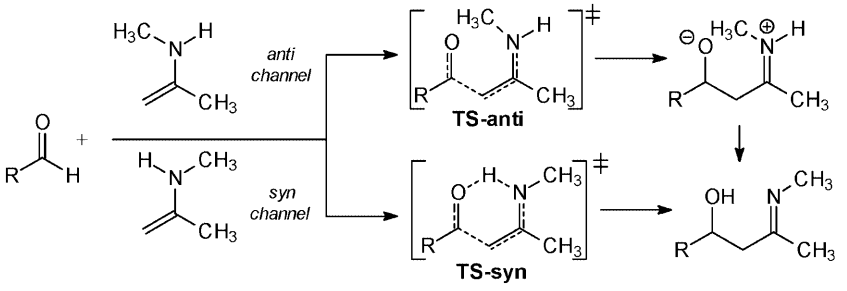


**Scheme 2**

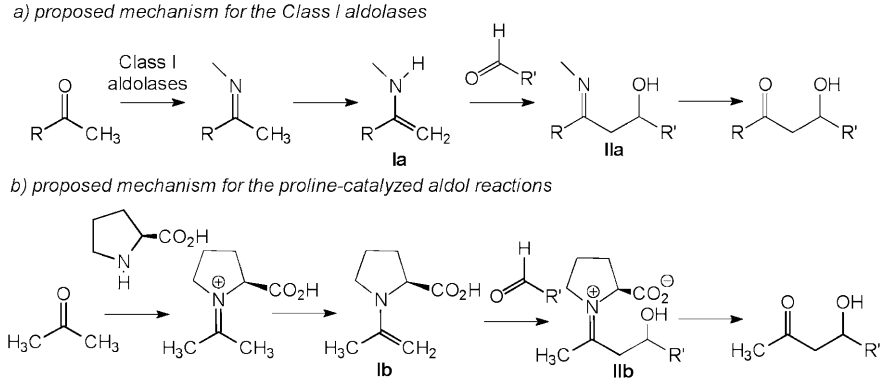


**Scheme 3**

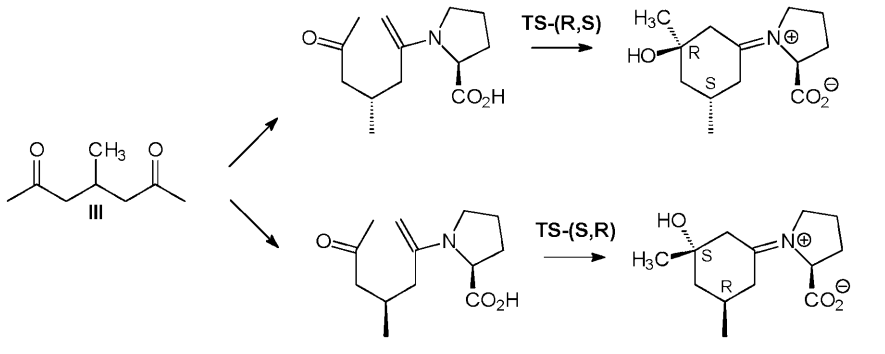


**Scheme 4**

aldol reaction (Scheme 4). This study denotes that the presence of an intramolecular hydrogen-bond between the carboxylic hydrogen atom and the alkoxide oxygen atom provides charge stabilization along the C—C bond-formation, it being responsible for the catalysis of these enamine-mediated aldol reactions [23, 27, 28]. For the proline-catalyzed intramolecular aldol reaction of the diketone **III**, the B3LYP/6-31G* energies for the diastereoisomeric TSs show that **TS-(R,S)** is preferred by 1 kcal/mol relative to **TS-(S,R)**, in reasonable agreement with experiment. The geometry of the proton transfer in the TSs determines the stereochemistry of this intramolecular process [27].

Our interest in the enzymatic-type catalyzed aldol reactions [28] has prompted us to carry out a theoretical investigation about the mechanism of the proline-catalyzed intermolecular aldol reaction using DFT [29, 30] with the well-established B3LYP/6-31G** method. We have investigated the mechanism and stereoselectivity for the C—C bond-formation step of the proline-catalyzed aldol reaction between acetone and isobutyraldehyde (**2**) in the presence of L-proline [20], as a model for these catalyzed reactions (Schemes 5, 6).

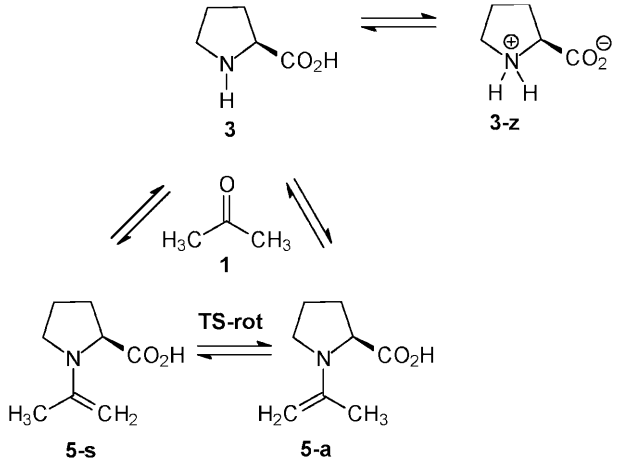


**Scheme 5**

## 2 Computational methods

DFT calculations were carried out using the B3LYP [31, 32] exchange-correlation functional, together with the standard 6-31G** basis set [33]. An exhaustive exploration of the potential-energy surfaces (PESs) was carried out to ensure that all relevant stationary points were located and properly characterized. The optimizations were carried out using the Berny analytical gradient optimization method [34]. The stationary points were characterized by frequency calculations in order to verify that minima and transition structures have zero and one imaginary frequency, respectively [35]. The intrinsic reaction coordinate (IRC) [36] paths were traced in order to check the energy profiles connecting each transition structure to the two associated minima of the proposed mechanism by using the second-order González–Schlegel integration method [37, 38]. The electronic structures of the stationary points were analyzed by the natural bond orbital method [39, 40]. All the calculations were carried out with the Gaussian 98 suite of programs [41]. The optimized geometries of all the stationary points on the PES are available from the authors.

These aldol reactions were carried out in polar solvents, and as solvents can modify both the gas-phase activation energy and stereoselectivity their effects were studied. The solvent effects were considered by optimizing the B3LYP/6-31G** gas-phase stationary points using a relatively simple self-consistent reaction field (SCRF) method [42, 43, 44] based on the polarizable continuum model of Tomasi's group [45, 46, 47]. The solvent used in the experimental was dimethyl sulfoxide (DMSO); therefore, we used its dielectric constant of 46.7.

## 3 Results and discussion

L-Proline-catalyzed aldol reactions involve enamine intermediates formed by condensation of carbonyl compounds with L-proline [19, 25, 48, 49, 50], and the rate-determining step of the reaction is the C—C bond-formation [25]. L-Proline can exist as two species in equilibrium (Scheme 5); the zwitterionic structure **3-z** is 0.6 kcal/mol less energetic than form **3**. With the inclusion of solvent effects (DMSO, $\varepsilon = 46.7$) this difference rises to 2.6 kcal/mol because of a large stabilization of the zwitterionic form. However, only structure **3** can yield the corresponding enamine by the nucleophilic attack of the N5 nitrogen atom of **3** to the carbonyl C2 carbon atom of acetone. For the enamine

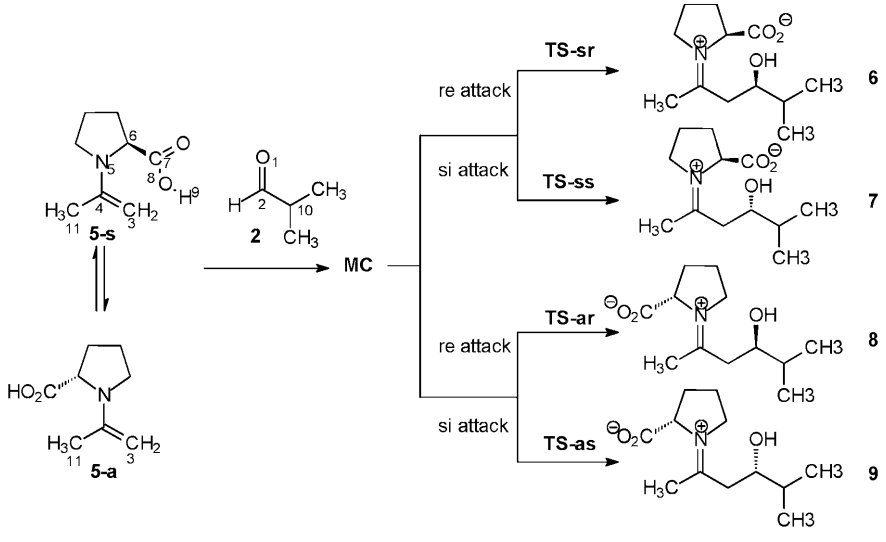


**Scheme 6**

two conformational structures, **5-s** and **5-a**, are possible owing to the restricted rotation around the C4–N5 single bond (Fig. 1). These conformers are related to the syn and anti arrangement of the active methylene group relative to the carboxylic acid group of L-proline. The conformer **5-s** is 1.0 kcal/mol (1.3 kcal/mol, $\varepsilon = 46.7$) less energetic that **5-a**; however, the easy C4–N5 bond-rotation, 8.0 kcal/mol (8.0 kcal/mol, $\varepsilon = 46.7$), allows the equilibration between these conformers. Unlike **3-z**, the zwitterionic forms of **5-s** and **5-a** are not stationary points in the gas phase; full optimization of the corresponding zwitterionic structures gives directly **5-s** and **5-a** without any appreciable barrier. Inclusion of solvent effects, DMSO, allows us to find the zwitterionic form of **5-s**, but it is 9.4 kcal/mol higher in energy. This behavior can be understood as a consequence of the large $sp^2$ character of the N5 nitrogen atom belonging to the vinylamine framework present in **5-a** and **5-s** that causes this nitrogen atom to be less basic. At L-proline this nitrogen atom has $sp^3$ hybridization.

The C—C bond-formation step also corresponds with the stereocontrol step for the proline-catalyzed reaction. For this step, four reactive channels have been studied. They are related to the nucleophilic attack of the C3 carbon atom of the active methylene group of the enamines **5-s** and **5-a** to the re and si faces of the carbonyl group of isobutyraldehyde, to give the zwitterionic iminium intermediates **6**–**9** (Scheme 6). After the hydrolysis, the iminium intermediates **6** and **8**, and **7** and **9** give (*R*)-cetol (**4**) and its enantiomer (*S*)-cetol, respectively. Thus, four TSs, **TS-sr**, **TS-ss**, **TS-ar** and **TS-as**, have been localized and characterized. They are related to the attack of active methylene of the enamines **5-s** and **5-a**, named as s and a, to the re and si faces of the carbonyl group of isobutyraldehyde, named as r and s. Associated with these TSs four zwitterionic iminium intermediates, **6**–**9**, have also been characterized. The geometries of four TSs are shown in Fig. 2, while the total and relative energies in vacuo and in DMSO are given in Table 1.

An IRC analysis from these TSs to reactants allows us to find several molecular complexes (MC) associated with an early stage of the C—C bond-formation process. At these species the O1 oxygen atom of isobutyraldehyde is hydrogen bonded to the acidic hydrogen atom of the carboxyl acid group of the L-proline residue. The easy bond rotation around the hydrogen-bond allows the equilibration between the MCs associated with each stereoisomeric reactive channel; the barrier for the bond rotation is 6.9 kcal/mol (6.1 kcal/mol, $\varepsilon = 46.7$). So, we considered only the MC associated with the attack of **5-a** to the re face of isobutyraldehyde, **MC**. This MC is about 5 kcal/mol more stable that the separated reactants.

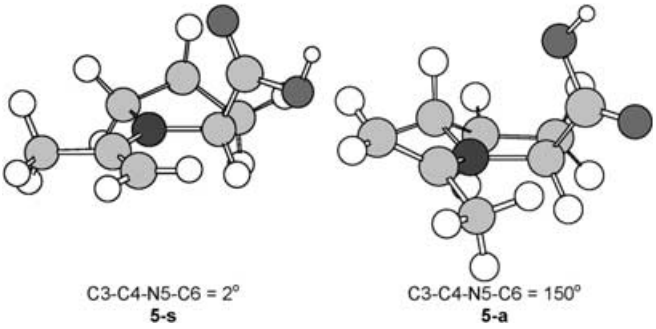


**Fig. 1.** Structures of the conformer enamines **5-s** and **5-a**

In the gas phase, the B3LYP/6–31G** barriers for the C—C bond-formation process, via **TS-sr**, **TS-ss**, **TS-ar** and **TS-as**, relative to **MC** are 14.4, 13.9, 9.6 and 11.0 kcal/mol, respectively. These barriers indicate that the reactive channels associated with the anti arrangement of the enamine are more favorable than those for the syn arrangement. In addition, for the anti channels the attack of the active methylene group of the enamine on the re face of the carbonyl group of isobutyraldehyde via **TS-ar** is 1.4 kcal/mol lower in energy than the attack on the si face via **TS-as**. This energetic result is in reasonable agreement with experiments where the (*R*)-cetol is isolated in 96% of enantiomeric excess, ee, (Scheme 1) [20]. Along the syn reactive channels **TS-ss** is 0.5 kcal/mol less energetic than **TS-sr**. Therefore, if the C—C bond-formation takes place along the syn arrangement of the enamine, **5-s**, the major stereoisomer will be the (*S*)-cetol in disagreement with experiment.

**Table 1.** Total energies (au) and relative energies (relative to **MC**) (kcal/mol, in *parentheses*) of the stationary points for the proline-catalyzed intermolecular aldol reaction between acetone (**1**) and isobutyraldehyde (**2**), in vacuo and in dimethyl sulfoxide (self-consistent reaction field, *SCRF*, $\varepsilon = 46.7$)

| | B3LYP/6-31G** | B3LYP/6-31G** SCRF | B3LYP/6-31 + G** SCRF// B3LYP/6-31G** SCRF |
|---|---|---|---|
| **2** | −232.470515 | −232.473903 | −232.484754 |
| **3** | −401.172153 | −401.180309 | −401.203214 |
| **3-z** | −401.173071 | −401.184453 | −401.206757 |
| **5-s** | −517.889673 | −517.897203 | −517.918893 |
| **5-a** | −517.888148 | −517.895140 | −517.917184 |
| **TS-rot** | −517.876920 | −517.884406 | −517.905629 |
| **MC** | −750.368861 | −750.377941 | −750.406974 |
| **TS-sr** | −750.345996 (14.4) | −750.357597 (12.8) | −750.384880 (13.9) |
| **TS-ss** | −750.346762 (13.9) | −750.358618 (12.1) | −750.387022 (12.5) |
| **TS-ar** | −750.353611 (9.6) | −750.366863 (7.0) | −750.395828 (7.0) |
| **TS-as** | −750.351393 (11.0) | −750.365481 (7.8) | −750.393620 (8.4) |
| **6** | −750.363566 (3.3) | −750.386443 (−5.3) | −750.418193 (−7.0) |
| **7** | −750.365832 (1.9) | −750.390417 (−7.8) | −750.424310 (−10.9) |
| **8** | −750.371907 (−1.9) | −750.393223 (−9.6) | −750.424718 (−11.1) |
| **9** | −750.368723 (0.1) | −750.389692 (−7.4) | −750.420887 (−8.7) |

These energetic results open the possibility that the Curtin–Hammett principle [51, 52] can be operative in this proline-catalyzed aldol reaction and, in consequence, the C—C bond-formation takes place via the more unfavorable anti arrangement, enamine **5-a**. These barriers are lower than that found for the C—C bond-formation step associated with the primary-amine-catalyzed aldol reaction (see **TS-syn** in the Introduction).

Inclusion of solvent effects, DMSO, stabilizes the MC, TSs and intermediates between 6–15 kcal/mol. The barriers for the C—C bond-formation along the more favorable anti channels decrease by about 3 kcal/mol owing to a larger solvatation of TSs than the MC (Table 1). The inclusion of solvent effects does not modify substantially the stereoselectivity found in the gas phase. In DMSO, **TS-as** is 0.8 kcal/mol more energetic than **TS-ar**. Finally, in DMSO the C—C bond-formation step is exothermic as a consequence of the large stabilization of the zwitterionic iminium intermediates.

Since some negative charge is located at all the stationary points, diffuse functions were used because of their superior ability to accommodate negative charges. The effects of the diffuse functions on the activation barriers and stereoselectivity were studied by single-point calculations at the B3LYP/6-31 + G** SCRF//B3LYP/6-31G** SCRF computational level. These calculations give the same enantioselectivity as found for the gas-phase B3LYP/6-31G** ones (Table 1); **TS-as** is 1.4 kcal/mol higher in energy than **TS-ar**. In addition, inclusion of diffuse functions does not modify the barriers obtained at the B3LYP/6-31G** SCRF level (Table 1). Therefore, for these hydrogen-bonded TSs the inclusion of diffuse functions does not modify the previous analysis.

The C—C bond-formation can also take place along the approach of isobutyraldehyde to the methylene C3 carbon atom of the enamines **5-a** and **5-s** through the opposite face of the molecular plane of L-proline containing the carboxylic acid group; however, these approach modes are very unfavorable owing to the nonstabilization of the negative charge that is developing at the carbonyl O1 oxygen atom along the C—C bond-formation. Thus, all attempts to locate the transition structure corresponding to the attack of the methylene of the enamine **5-a** to the si face of isobutyraldehyde to give the alkoxide–iminium intermediate (**8′**) were unsuccessful (Scheme 7). Restricted optimization freezing the C2–C3 distance to 1.8 Å leads to a structure that is about 18 kcal/mol more energetic than **TS-ar** (Fig. 3). In addition, the corresponding alkoxide intermediate **8′** cannot be obtained as a stationary point [28]. A similar result is found for the primary-amine-catalyzed aldol reaction where the **TS-anti** is about 16 kcal/mol more energetic than the **TS-syn**.

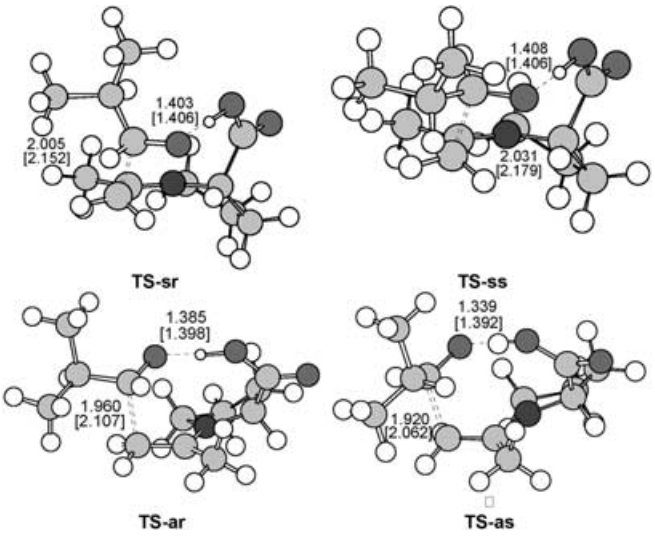


**Fig. 2.** Transition structures corresponding to the C—C bond-formation process for the proline-catalyzed intermolecular aldol reaction between **1** and **2**. The values of the lengths of the bonds directly involved in the reaction obtained at the B3LYP/6-31G**. and B3LYP/6-31G** in dimethyl sulfoxide (in brackets) levels are given in angstroms

Therefore, the intermolecular hydrogen-bond in the proline-catalyzed process is responsible for the large catalytic effect observed for this kind of catalyzed aldol reaction. In addition, the barrier for the C—C bond-formation in this L-proline-catalyzed process is lower than that found in the primary-amine-catalyzed process as a consequence of the more acidic character of the COOH hydrogen atom of L-proline than the NH hydrogen atom of the enamine. This large acidic character stabilizes more effectively the negative charge that is developing at the carbonyl O1 oxygen atom along the nucleophilic attack.

Analysis of the geometrical parameters for enamines **5-s** and **5-a** shows that the N5 nitrogen atom has nearly $sp^2$ hybridization. The C4–N5–C6 bond angles for **5-s** and **5-a** are about 122°. This $sp^2$ hybridization that allows a favorable interaction between the N5 lone pair and the neighboring C3–C4 double bond allows us to explain the lower basic character of the N5 nitrogen atom for these enamines relative to the pyramidalized N5 nitrogen atom in L-proline. The C3–C4–N5–C6 dihedral angle for **5-a**, 150°, shows a large deviation of the plane of the C3–C4 double bond relative to the $sp^2$ plane of the N5 nitrogen atom as a consequence of steric hindrance between the C11 methyl group and the carboxylic acid group present on L-proline (Fig. 1). Therefore, this hindrance is responsible for the larger energy of **5-a** relative to **5-s**.

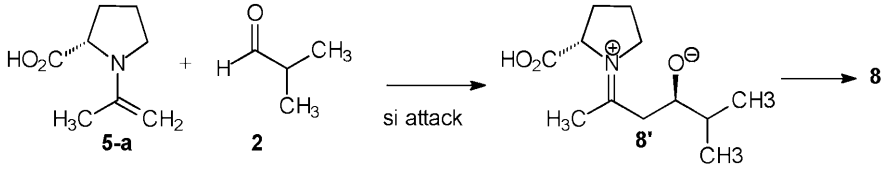


**Scheme 7**

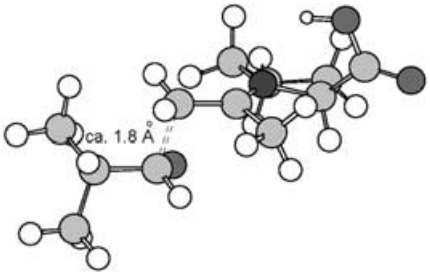


**Fig. 3.** Approximation to the transition structure corresponding to the C—C bond-formation process along the opposite face of the acid carboxylic group

Along the C—C bond-formation the lengths of the C2–C3 forming bond at **TS-sr**, **TS-ss**, **TS-ar** and **TS-as** are 2.005, 2.031, 1.960 and 1.920 Å, respectively. The lengths at the more favorable anti TSs are similar to that found for the more favorable syn reactive channel for the primary-amine-catalyzed aldol reaction (1.944 Å at **TS-syn** in Scheme 2). The O1–H9 and O8–H9 lengths at these TSs are 1.403 and 1.059 Å at **TS-sr**, 1.408 and 1.060 Å at **TS-ss**, 1.385 and 1.080 Å at **TS-ar** and 1.339 and 1.081 Å at **TS-as**, respectively. At **MC** these values are 1.807 and 0.987 Å, respectively. These lengths indicate that the O8–H9 bond breaking is much delayed at these TSs [28].

Inclusion of solvent effects on the optimization does not modify substantially the gas-phase geometries (Fig. 2). The lengths of the C2–C3 forming bond are slightly larger than those obtained in the gas phase. Therefore, with the inclusion of solvent effects the C—C bond-formation process is slightly earlier.

A conformational analysis of the C2–C3 forming bond at the more favorable anti TSs shows that while **TS-ar** presents a gauche arrangement between the carbonyl oxygen atom and the enamine framework, the O1–C2–C3–C4 dihedral angle is 46°, the more unfavorable **TS-as** presents two gauche arrangements, the O1–C2–C3–C4 and C10–C2–C3–C4 dihedral angles are 46° and −83°, respectively (Fig. 4). Therefore, the steric hindrance that appear between the isopropyl group belonging to isobutyraldehyde and the methyl group of enamine **5-a** at **TS-as** is responsible for the larger energy of the latter relative to **TS-ar** and, in consequence, for the enantioselectivity shown for this proline-catalyzed intermolecular aldol reaction. The C10–C2–C3–C4 dihedral angle at the more favorable **TS-ar** is 170°.

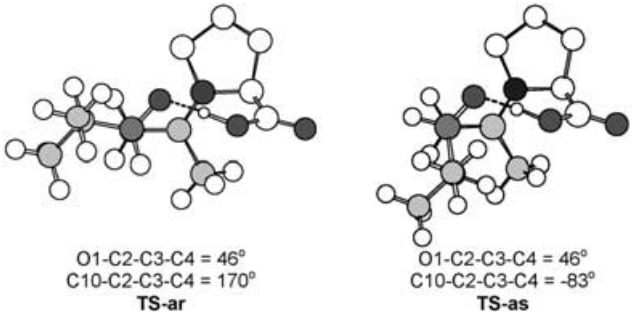


**Fig. 4.** Anti and gauche arrangement of the isopropyl group, C10–C2–C3–C4 dihedral angles, along the C—C bond-formation at the more favorable **TS-ar** and **TS-as**, respectively

The values of the unique imaginary frequency associated with **TS-sr**, **TS-ss**, **TS-ar** and **TS-as** are 326*i*, 313*i*, 326*i* and 430*i* $cm^{-1}$, respectively. Analysis of the atomic movement associated with these imaginary frequency indicates that these TSs are associated mainly with the movement of the C2 and C3 carbon atoms along the C2–C3 bond-formation and the coupled movement of the acidic H9 hydrogen atom along the proton-transfer process; therefore, the C2–C3 bond-formation and the proton transfer are concerted processes at these TSs.

The Wiberg bond order (BO) [53] values of the C2–C3 forming bond at **TS-sr**, **TS-ss**, **TS-ar** and **TS-as** are 0.49, 0.47, 0.52 and 0.56, respectively. The more favorable anti TSs are slightly more advanced than the syn ones. These BOs are similar to those found for the C—C bond-formation for the primary-amine-catalyzed aldol reaction. The BO values of the O1–H9 and O8–H9 bonds at these TSs are 0.23 and 0.51 at **TS-sr**, 0.21 and 0.50 at **TS-ss**, 0.23 and 0.48 at **TS-ar** and 0.27 and 0.44 at **TS-as**, respectively. The O8–H9 BO value at the TSs is slightly lower than that at **MC**, 0.64. Therefore, the proton-transfer process is more delayed than the C—C bond-formation one [28]. Finally, the BO value of the C4–N5 bond at these TSs, about 1.35, indicates a large $\pi$ character for the C4–N5 single bond as a consequence of the large participation of the N5 lone pair in the C—C bond-formation process; at **MC** the C4–N5 BO is 1.11.

Finally, the natural population analysis [39] allows us to evaluate the charge transfer along the C—C bond-formation process. An analysis of the natural charges at the atoms belonging to the carbonyl group, O1 and C2, at the corresponding MC and the TSs allows us to evaluate the charge transfer at the TSs along the nucleophilic attack of enamines **5-s** and **5-a** to isobutyraldehyde (Table 2). The charges transferred to the carbonyl group at the TSs are 0.32*e* at **TS-sr**, 0.31*e* at **TS-ss**, 0.38*e* at **TS-ar** and 0.40*e* at **TS-as**; therefore, there is a larger charge transfer at the more favorable anti TSs than at the syn ones. These results agree with the larger C—C bond-formation found at the anti TSs than at the syn ones (see bond lengths and BO analysis). In addition the C2–C3 bond-formation process at **TS-as** is slightly more advanced than that at **TS-ar**. However, the steric hindrance that appears between the isopropyl group of isobutyraldehyde and the methyl group of enamine **5-a** at **TS-as** is responsible for the larger energy of the latter

**Table 2.** Natural charges and charge transfer (au) to the carbonyl group in the proline-catalyzed aldol reaction between **1** and **2**

| | MC | TS-sr | TS-ss | TS-ar | TS-as |
|---|---|---|---|---|---|
| | Natural charges | | | | |
| O1 | −0.57 | −0.73 | −0.73 | −0.76 | −0.77 |
| C2 | 0.45 | 0.29 | 0.29 | 0.26 | 0.25 |
| C3 | −0.59 | −0.62 | −0.62 | −0.59 | −0.58 |
| C4 | 0.20 | 0.33 | 0.33 | 0.36 | 0.36 |
| N5 | −0.48 | −0.38 | −0.38 | −0.38 | −0.38 |
| | Charges on groups | | | | |
| C═O | −0.12 | −0.44 | −0.43 | −0.50 | −0.52 |
| N—C═C | −0.88 | −0.67 | −0.67 | −0.62 | −0.60 |
| | Charge transfer to the carbonyl group | | | | |
| | | −0.32 | −0.31 | −0.38 | −0.40 |

relative to **TS-ar** and, in consequence, for the observed enantioselectivity.

## 4 Conclusions

The transition structures associated with the C—C bond-formation step of the proline-catalyzed intermolecular aldol reaction between acetone and isobutyraldehyde have been studies using DFT methods at the B3LYP/6-31G** computational level. Reaction of acetone with L-proline affords an enamine that is in equilibrium between two planar conformations. The subsequent nucleophilic attack of the active methylene of the enamine to the carbonyl group of isobutyraldehyde yields an iminium–alcohol intermediate along the C—C bond-formation. For this step, which is the stereo-controlling and rate-determining step, four reactive channels corresponding to the syn and anti arrangement of the active methylene of the enamine relative to the carboxylic acid group of L-proline and the two diastereoisomeric approach modes to the re and si faces of the carbonyl group of the aldehyde were studied. Formation of an intermolecular hydrogen-bond between the acidic hydrogen of L-proline and the carbonyl oxygen atom of the aldehyde in an early stage of the process catalyzes very effectively the C—C bond-formation by a large stabilization of the negative charge that is developing at the carbonyl oxygen atom along the nucleophilic attack. As a consequence of the hydrogen-bond formation, the reactive channels associated with the anti arrangement of the enamine are favored over the channels associated with the syn arrangement. In addition, along the anti channels the attack of the active methylene on the re face of the aldehyde is favored over the attack on the si face, in agreement with experiment. Inclusion of solvent effects, DMSO, reduces the barrier heights by the larger solvation of the TSs than the reactants. This DFT study is in complete agreement with experiments, allowing us to explain the origin of the catalysis and stereoselectivity in these L-proline-catalyzed aldol reactions.

*Acknowledgements.* This work was supported by research funds provided by the Ministerio de Educación y Cultura of the Spanish Government by DGICYT (project PB98–1429). All the calculations were performed on a Cray–Silicon Graphics Origin 2000 of the Servicio de Informática de la Universidad de Valencia. We are most indebted to this center for providing us with computer capabilities.

## References

1. Masamune S, Choy W, Peterson JS, Sita LR (1985) Angew Chem Int Ed Engl 24:1
2. Heathcock CH (1990) Aldrichim Acta 23:99
3. Evans DA (1988) Science 240:420
4. Cowden CJ, Paterson I (1997) Org React 51:1
5. Franklin AS, Paterson I (1994) Contemp Org Synth 1:317
6. Nelson SG (1998) Tetrahedron Asymmetry 9:357
7. Yanagisawa A, Matsumoto Y, Nakashima H, Asakawa K, Yamamoto H (1997) J Am Chem Soc 119:9319
8. Carreira EM, Lee W, Singer RA (1995) J Am Chem Soc 117:3649
9. Evans DA, MacMillan DWC, Campos KR (1997) J Am Chem Soc 119:10859
10. Ager DJ, East MB (1996) Asymmetric synthetic methodology. CRC, Boca Raton
11. Wong CH, Whiteside GM (1994) Enzymes in synthetic organic chemistry. Pergamon, Oxford
12. Wong CH, Halcomb RL, Ichikawa Y, Kajimoto T (1995) Angew Chem Int Ed Engl 34:412
13. Fessner WD (1998) Curr Opin Chem Biol 2:85
14. Machajewski TD, Wong CF (2000) Angew Chem Int Ed Engl 39:1352
15. Wagner J, Lerner RA, Barbas CF III (1995) Science 270:1797
16. Barbas CF III, Heine A, Zhong G, Hoffmann T, Gramatikova S, Björnestedt R, List B, Anderson J, Stura EA, Wilson EA, Lerner RA (1997) Science 278:2085
17. Hoffmann T, Zhong G, List B, Shabat D, Anderson J, Gramatikova S, Lerner RA, Barbas CF III (1998) J Am Chem Soc 120:2768
18. Zhong G, Hoffmann T, Lerner RA, Danishefsky S, Barbas CF III (1997) J Am Chem Soc 119:8131
19. List B, Lerner RA, Barbas CF III (1999) Org Lett 1:59
20. List B, Lerner RA, Barbas CF III (2000) J Am Chem Soc 122:2395
21. Ahrendt KA, Borths CJ, MacMillan DWC (2000) J Am Chem Soc 122:4243
22. Jen WS, Wiener JJM, MacMillan DWC (2000) J Am Chem Soc 122:9874
23. Bahmanyar S, Houk KN (2001) J Am Chem Soc 123:11273
24. Reymond JL, Chen Y (1995) J Org Chem 60:6970
25. Reymond JL (1998) J Mol Catal B 5:331
26. Groger H, Wilken J (2001) Angew Chem Int Ed Engl 40:529
27. Bahmanyar S, Houk KN (2001) J Am Chem Soc 123:12911
28. Arno M, Domingo LR (2001) Int J Quantum Chem 83:338
29. Parr RG, Yang W (1989) Density functional theory of atoms and molecules. Oxford University Press, New York
30. Ziegler T (1991) Chem Rev 91:651
31. Becke AD (1993) J Chem Phys 98:5648
32. Lee C, Yang W, Parr RG (1988) Phys Rev B 37:785
33. Hehre WJ, Radom L, Schleyer PvR, Pople JA (1986) Ab initio molecular orbital theory. Wiley, New York
34. Schlegel HB (1994) In: Yarkony DR (ed) Modern electronic structure theory. World Scientific Publishing, Singapore
35. Tapia O, Andres J (1984) Chem Phys Lett 109:471
36. Fukui K (1970) J Phys Chem 74:4161
37. Gonzalez C, Schlegel HB (1990) J Phys Chem 94:5523
38. Gonzalez C, Schlegel HB (1991) J Chem Phys 95:5853
39. Reed AE, Weinstock RB, Weinhold F (1985) J Chem Phys 83:735
40. Reed AE, Curtiss LA, Weinhold F (1988) Chem Rev 88:899
41. Frisch MJ, Trucks GW, Schlegel HB, Scuseria GE, Robb MA, Cheeseman JR, Zakrzewski VG, Montgomery JA Jr, Stratmann RE, Burant JC, Dapprich S, Millam JM, Daniels AD, Kudin KN, Strain MC, Farkas O, Tomasi J, Barone V, Cossi M, Cammi R, Mennucci B, Pomelli C, Adamo C, Clifford S, Ochterski J, Petersson GA, Ayala PY, Cui Q, Morokuma K, Malick DK, Rabuck AD, Raghavachari K, Foresman JB, Cioslowski J, Ortiz JV, Stefanov BB, Liu G, Liashenko A, Piskorz P, Komaromi I, Gomperts R, Martin RL, Fox DJ, Keith T, Al-Laham MA, Peng CY, Nanayakkara A, Challacombe M, W Gill PM, Johnson B, Chen W, Wong MW, Andres JL, Gonzalez C, Head-Gordon M, Replogle ES, Pople JA (1998) Gaussian 98, revision A6. Gaussian, Pittsburgh, Pa
42. Tapia O (1992) J Math Chem 10:139
43. Tomasi J, Persico M (1994) Chem Rev 94:2027
44. Simkin BY, Sheikhet I (1995) Quantum chemical and statistical theory of solutions - A computational approach. Horwood, London
45. Cances MT, Mennunci V, Tomasi J (1997) J Chem Phys 107:3032
46. Cossi M, Barone V, Cammi R, Tomasi J (1996) Chem Phys Lett 255:327

47. Barone V, Cossi M, Tomasi J (1998) J Comput Chem 19:404
48. Agami C (1988) Bull Soc Chim Fr 499
49. Agami C, Platzer N, Sevestre H (1987) Bull Soc Chim Fr 358
50. Brown KL, Damm L, Dunitz JD, Eschenmoser A, Hobi R, Kratky C (1978) Helv Chim Acta 3108
51. Curtin DY (1954) Rec Chem Prog 14:111
52. Hammett LP (1970) Physical organic chemistry. McGraw-Hill, New York, chap 5
53. Wiberg KB (1968) Tetrahedron 24:1083